BS17 MOLECULAR MRI OF COLLAGEN III DETECTS CARDIAC FIBROSIS AND TREATMENT RESPONSE

[1]Nadia Chaher*, [1]Giuseppe Digilio, [2]Sara Lacerda, [1]Ling Gao, [3]Begoña Plaza, [1]Carlos Velasco, [4]Gastao Cruz, [1]Claudia Prieto, [1]René Botnar, [1]Alkystis Phinikaridou. *[1]King's College London, St Thomas Hospital, London, LND SE1 7EH, UK; [2]University of Turin; [3]Centre de Biophysique Moléculaire; [4]Complutense University of Mardrid; [5]University of Michigan*

10.1136/heartjnl-2024-BCS.243

Introduction Heart failure (HF) has reached epidemic proportions, affecting about 64 million people globally and is the main cause of death and disability[1]. Cardiac fibrosis, characterised by changes in type I (COL1) and III (COL3) collagen, drive HF[2,3]. After a myocardial infarction (MI), both COL1 and COL3 increase in the infarcted myocardium[4]. COL3 increases in the early stages of remodelling, and it is later replaced by COL1[5]. Non-invasive methods to selectively image and quantify collagen lacking or limited to COL1. Here, we developed and used an imaging probe that specifically binds to COL3 to image remodelling after MI and used it as a tool to detect enalapril, an ACE inhibitor commonly used to treat HF patients, treatment response.

Method Previously we developed a COL3-binding probe and demonstrated the probes' high affinity and specificity[6]. Here, we labelled the probe with Gadolinium [Gd(III)] for in vivo CMR studies. In vivo functional and molecular CMR was performed using a 3 Tesla clinical scanner at days 10 and 21 post-MI (n=6/ group). The same mice were imaged the next day with a negative control probe, and again the next day with Gadovist (n=3) for comparison. The COL3-probe was used as a tool to monitor the effect of enalapril on myocardial fibrosis after MI. Mice were administered enalapril (20 mg/kg/day) immediately after MI and imaged at days 10 and 21 (n=6/ group). 2D short axis cine images covering the left ventricle (LV) were used to assess cardiac function parameters including ejection fraction (EF,%). T1-weighted 3D inversion recovery (IR) images were used to acquire Late Gadolinium Enhancement (LGE) images of the LV 60 min after intravenous injection of the probe (0.2 mmol/kg). T1 mapping was performed using a 2D Look-Locker sequence with an inversion pulse applied followed by the acquisition of 30 inversion recovery.

Results Molecular CMR enabled selective profiling of the natural turnover of COL3 after MI with the signal increasing at day 10, when COL3 is elevated, and decreasing at day 21 as COL3 is replaced by COL1 (Fig.1A). The imaging data were validated by histology showing co-localisation of the MRI signal with COL3 (green) at day 10 and reduction at day 21. Quantitative T1 maps discriminated between infarcted and remote myocardium with lower T1 values in the infarct and higher in the remote myocardium. No enhancement was observed using the control probe or the clinical agent Gadovist. Mice receiving enalapril showed similar enhancement at day 10 compared to untreated mice (Fig. 1B). However, at day 21 mice treated with enalapril showed a significantly higher LGE volume compared with untreated mice (Fig. 1B), indicating that enalapril may prolong the accumulation of COL3 (Fig. 1C). However, despite changes in the COL3 observed with molecular imaging, cardiac function was similar between the groups (Fig.1D) suggesting that molecular changes may precede functional changes.

Discussion We have developed the first probe suitable for molecular imaging of COL3. Combining this probe with quantitative CMR, enabled imaging of previously undetectable changes in COL3 remodelling after myocardial infarction and in response to treatment. This could address a considerable knowledge gap in the roles of COL3 in cardiac fibrosis. Our

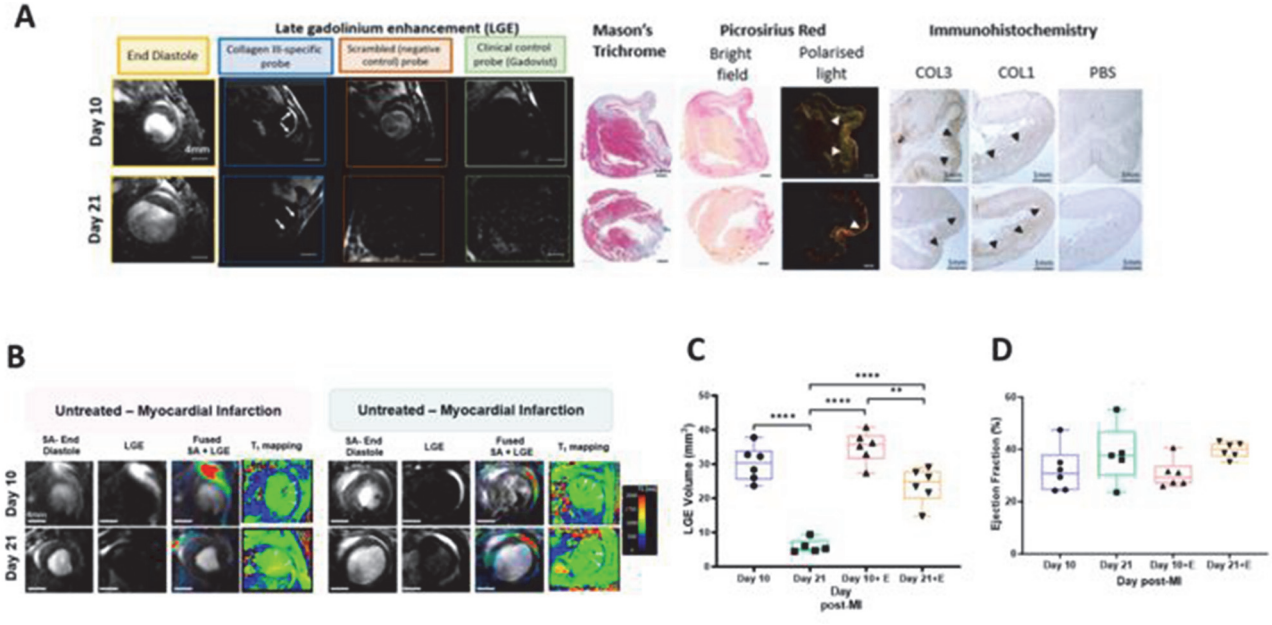

Abstract BS17 Figure 1 First *in vivo* CMR using the COL3-specific imaging probe and using it to investigate the effects of enalapril on COL3 remodelling. A. Increased signal enhancement in the infarcted myocardium at day 10 that decreased by day 21 which co-localised with COL3 as seen by histology. Importantly no enhancement was observed with both the negative control probe and the non-targeted clinical probe. **B.** Similar signal enhancement (SE) in the infarcted myocardium at day 10 following MI. However, at day 21 treated mice showed higher SE compared with untreated mice. **C.** Quantification of the LGE volume verified the observations in panel B. **D.** There was no significant difference in cardiac function between both groups (where P value of *=0.033, **=0.021, ***=0.002 and ****=0.0001)

approach may provide a new tool to investigate the imaging, therapeutic and functional roles of COL3 in myocardial fibrosis non-invasively that remain elusive.
Conflict of Interest None

BS18 DEVELOPMENT AND VALIDATION OF DECONVOLUTION METHODS FOR BULK RNA-SEQ DATA ANALYSIS IN HUMAN MYOCARDIUM AND SKELETAL MUSCLE USING CIBERSORTX

[1]Marcella Conning-Rowland*, [1]Chew Cheng, [1]Marilena Giannoudi, [2]Eylem Levelt, [1]Lee Roberts, [1]Kathryn Griffin, [3]Richard Cubbon. *[1]Leeds Institute of Cardiovascular and Metabolic Medicine, The University of Leeds, Light Laboratories,, 6 Clarendon Way, Leeds, WYK LS2 3AA, UK; [2]University of Leeds, Leeds Institute of Cardiovascular and Metabolic Medicine, LS2 9JT, United Kingd; [3]University of Leeds*

10.1136/heartjnl-2024-BCS.244

Single-cell RNA-seq is a vital tool for deciphering patterns of gene expression within the multitude of cell lineages comprising any tissue. However, price and technical complexities limit the use of this technology. Deconvolution of bulk RNA-seq data from whole tissues offers an alternative approach to derive some of these insights and gain valuable contextual information from existing data.

Cardiovascular diseases and their risk factors alter myocardial and skeletal muscle biology. We aimed to develop and validate approaches to deconvolute bulk RNAseq data from human right atrium (RA), left ventricle (LV) and skeletal muscle biopsies, allowing inference of the cellular composition of these samples.
Methods We used single-cell RNA-seq data from the Heart Cell Atlas project to construct signature matrices encompassing all major cell lineages using the CIBERSORTx deconvolution package. Randomly selecting 200 cells from each cell lineage, we generated a signature matrix for each tissue, including fibroblasts, endothelial cells, lymphoid cells, myeloid cells, neuronal cells, pericytes, smooth muscle cells, and myocytes (defined as atrial cardiomyocytes and ventricular cardiomyocytes in the RA and LV matrices, respectively). Cardiac signature matrices also included adipocytes and neuronal cells, while the skeletal muscle signature matrix also incorporated satellite cells. These matrices can be applied in CIBERSORTx by any scientist wishing to infer cell lineage proportions in their bulk RNAseq data.

To assess the accuracy of these signature matrices, we generated 100 synthetic RA, LV and skeletal muscle datasets with varying proportions of each cell lineage and compared their known composition with the composition predicted by CIBERSORTx. To illustrate their value in deconvolution, we applied our signature matrices to publicly available bulk RNA-seq data from the Genotype Tissue Expression (GTEx) project to explore the association of age and sex with cellular composition of these tissues.
Results Linear regression analyses revealed excellent agreement between known and predicted composition of synthetic tissues, with $R2>0.95$ for all cell lineages, and good calibration. Deconvolution of skeletal muscle data from GTEx revealed, amongst other differences, a lower proportion of satellite cells and a higher proportion of fibroblasts with age, both of which have been demonstrated previously using alternative methods, corroborating the accuracy of our approach. Wide-ranging age- and/or sex- differences were noted in all tissues, which warrant further assessment using complementary approaches.
Conclusions Our validated CIBERSORTx signature matrices represent user-friendly tools for elucidating how disease processes influence cell lineage composition of human myocardium and skeletal muscle. These allow additional insights to be gained from existing and new bulk RNAseq data, which may help to define important cell lineages for further characterisation using complementary approaches.
Conflict of Interest None

BS19 DIAGNOSTIC 12-LEAD ECG RECORDINGS IN THE 3-TESLA CMR BORE AT REST AND DURING ADENOSINE STRESS PERFUSION- RESULTS FROM MYOFIT46

[1]Debbie Falconer*, [1]Maroua Mehri, [2]Mohammed Bhiri, [1]Isabelle Whitmore, [1]Emma Martin, [1]Lee Hamil-Howes, [1]Alicja Rapala, [1]Matthew Webber, [2]Fiona Chan, [1]Cristian Topriceanu, [1]Pier Lambiase, [1]Nish Chaturvedi, [1]Peter Kellman, [1]James Moon, [1]Iain Pierce, [1]Alun Hughes, [2]Guillaume Calmon, [1]Gabriella Captur. *[1]University College London, Roger Williams Building, Chenies Mews, London, LND WC1E 6HX, UK; [2]Epsidy; [3]Univesity College London*

10.1136/heartjnl-2024-BCS.245

Background Current electrocardiographic (ECG) devices built into cardiovascular magnetic resonance (CMR) scanners have a narrow bandwidth (0.5–60Hz) and signals suffer from distortion due to magnetic field gradient artefact and magnetohydrodynamic effects, so ECGs are non-diagnostic except for R-peak detection. Despite advanced QRS detection algorithms, incorrect R peak detection hampers image acquisition, especially at higher field strengths, thus prolonging scan time and producing suboptimal images. Previous feasibility studies at 1.5 and 3 Tesla (T) using external ECG devices were small: n=14 and n=4 healthy volunteers respectively. We implemented a novel hardware and software system for integrating an external device into a clinical 3T CMR scanner to derive diagnostic 12-lead ECGs from inside the scanner bore and during stress perfusion acquisition.
Methods Standard 12-lead ECGs were first recorded on participants of the MyoFit46 cardiovascular sub-study of the National Survey of Health and Development outside the CMR environment using conventional electrode placement. CMR was then performed using Siemens Prisma 3T magnet. Three electrodes (each with 3 measurement and 1 reference electrodes, Fig1a) were applied to the chest of participants. Short leads connected each electrode to a sensor for signal amplification and digitalisation (Fig1b). Signals were then transmitted via 10 m-long dual fibre-optic cables running through a penetration hole into the adjacent room to reach an electronics signal module and connected laptop (32 cores,5.2GHz) equipped with easyG/truzyG/Epsidy software (Fig1c). ECGs were recorded for 30 seconds prior to image acquisition in all participants and repeated during stress perfusion acquisition in one participant as proof-of-principle. Post-processing denoise filtering removed gradient artefact and a subject-specific matrix was applied to reconstruct 12-lead ECGs from the raw signal. The morphology of each beat of the in-bore 12-lead ECG was compared to the reference ECG (outside the scanner) using Pearson's correlation coefficient on the PQRST waveform.
Results 20 participants were prospectively recruited (60% male, 76±0 years). In-bore 12-lead ECGs were safe and